HAL open science

Modelling the age of ice of Aletsch glacier

Claire-Mathilde Stucki, Guillaume Jouvet

▶ To cite this version:

Claire-Mathilde Stucki, Guillaume Jouvet. Modelling the age of ice of Aletsch glacier. Université de Lausanne. 2024. hal-04663408

HAL Id: hal-04663408
https://hal.science/hal-04663408v1

Submitted on 27 Jul 2024

HAL is a multi-disciplinary open access archive for the deposit and dissemination of scientific research documents, whether they are published or not. The documents may come from teaching and research institutions in France or abroad, or from public or private research centers.

L'archive ouverte pluridisciplinaire **HAL**, est destinée au dépôt et à la diffusion de documents scientifiques de niveau recherche, publiés ou non, émanant des établissements d'enseignement et de recherche français ou étrangers, des laboratoires publics ou privés.

Distributed under a Creative Commons Attribution - NonCommercial - ShareAlike 4.0 International License

Modelling the age of ice of Aletsch glacier

Claire-Mathilde Stucki

Research internship - First year of IJC master
April 2nd to July 26th, 2024

ICE Group (Interaction between Climate and Environment)
Institut des dynamiques de la suface terrestre (IDYST)
University of Lausanne
Geopolis Building, UNIL Mouline, 1015 Lausanne, Switzerland

Work supervised by Guillaume Jouvet

Figure 1: Satellite view of Aletsch glacier, Switzerland. Source : retorte.ch/map

Contents

Abstract

in English

Aletsch glacier is the greatest glacier of the Alps. It has been modelled several times in order to reproduct its past behaviour and predict its future evolution. Although, the age of the ice constituting this glacier has never been studied. Data allowing to date a specific area of the glacier are provided by nuclear tests realised during cold war. The ice dating from the Cold War has been contaminated by radionuclides dispersed during these tests, and its current position can therefore be determined by measuring radioactivity. The aim of this study is to use these data in order to calibrate a numerical model of Aletsch glacier including a lagrangian age of ice modelling. It allows to map the age of the ice. We found that the oldest ice is located at the base of the glacier and dates from between 1000 or 1500. This uncertainty comes from the value of the basal sliding of the glacier which is not well known. On surface of the glacier, the basal sliding has much less influence on the age model result. The surface ice dates from between 1700 for the bottom of the ablation area and present time for the accumulation area. These results suggest that basal sliding should be further studied in order to constrain the model more precisely.

in French

Le glacier d'Aletsch est le plus grand glacier des Alpes. Il a déjà été modélisé à plusieurs reprises pour reproduire son comportement passé et prédire son évolution future. Cependant, l'âge de la glace constituant le glacier n'a jamais été étudiée. Les essais nucléaires réalisés pendant la guerre froide fournissent des données permettant de dater une partie du glacier. En effet, la glace datant de la guerre froide a été contaminée par les radionucléides dispersés lors de ces essais, et l'on peut donc retrouver sa position actuelle par des mesures de radioactivité. Le but de cette étude est d'utiliser ces données pour calibrer un modèle numérique du glacier d'Aletsch incluant une modélisation lagrangienne de l'âge de la glace. Cela permet de cartographier l'âge de la glace. Nous avons trouvé que la glace la plus ancienne se situe à la base du glacier et date d'entre 1000 et 1500. Cette incertitude vient de la valeur du glissement basal, qui est mal connue. À la surface du glacier, le glissement basal a très peu d'influence sur le résultat du modèle d'âge. La glace de surface date d'environ 1700 pour le bas de la zone d'ablation et d'aujourd'hui pour la zone d'accumulation. Ces résultats suggèrent que le glissement basal a un effet important sur la dynamique de la glace et devrait être davantage étudié afin de contraindre le modèle de manière plus précise.

1 Introduction to glacial processes

Climate change is causing glaciers and ice caps to retreat. This retreat has a strong influence on the evolution of landscapes and is a source of natural disasters that can affect the safety of populations, tourism and the economy. There is therefore a major interest in understanding and predicting the mechanisms governing the movement and evolution of glaciers [Marzeion et al., 2018].

A glacier is a mass of ice formed by the accumulation and compression of snow under its own weight. Under the effect of gravity, this ice undergoes a deformation and flows along the bedrock on which it lies exactly like a highly viscous fluid, even though it is a solid. At higher altitude, the temperature is colder and snow accumulates to form new ice. In the lower zone of the glacier, at lower altitude, the temperature is higher and the ice melts and sublimates: this is known as ablation. These processes are summarised in figure 2. The equilibrium line of a glacier is defined as the position where accumulation and ablation exactly compensate each other. The raising or lowering of this line over time is a sign of the glacier's advance or retreat.

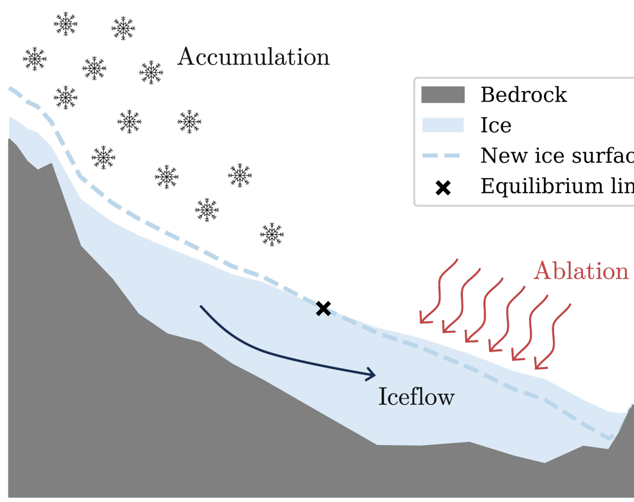

Figure 2: Schematic view of a glacier and its main processes

Glaciologists use physical models to study and quantify the processes governing the evolution of glaciers [Glen, 1953]. Ice dynamics is described using fluid dynamics and, more specifically, the Stokes equation, which is an approximation of the Navier-Stokes equation for cases of very high viscosity. The amount of accumulation and melting are summarised in the surface mass balance (SMB). This quantity is positive where there is ice accumulation and negative where there is ablation. The glacier's equilibrium line corresponds to all the points where the SMB is zero. The equilibrium line altitude (ELA) provides a simplified description of the SMB. It is therefore possible to describe the evolution of glaciers using physical equations, but these cannot be solved analytically because the actual topography and climate forcing are too complex. This is why glaciologists use numerical modelling.

Glaciers have traditionally been modelled using finite element schemes which require significant computing power and time to run the simulations. Recent advances in physically informed neural networks have enabled the development of a new type of glacier model that uses a neural network instead of completely solving the physical equations. They make it easier to carry out simulations. With traditional models, it takes several hours or days of computing on supercomputers to simulate a glacier over several hundred years. With models using deep learning, this can now be done on a laptop in a few minutes [Jouvet and Cordonnier, 2023].

2 Aim of the internship

The Aletsch glacier (Figure 1) is the largest glacier in the Alps. It consists of three high-altitude glaciers, called accumulation basins, merging together into a final tongue. It is around 20 kilo m long and reaches a maximum thickness of 900 m. Because of this special status, a lot of data is available for this glacier [Jouvet et al., 2011], but the age of the ice has never been fully studied. To date the ice, field data about the age of ice is required. Such data are provided by the position of the ice contaminated by radionuclides. During the Cold War, nuclear tests were carried out, depositing radionuclides on the Earth's surface, including on the Aletsch glacier. These radionuclides were trapped in the ice and have since followed its movement. By measuring nuclear activity at different positions on the glacier, it is possible to determine the current position of the ice that was contaminated during the Cold War. In 2020, a measurement campaign was carried out on the Aletsch glacier for this purpose. The aim of this internship is to use the resulting data to calibrate a numerical model of the Aletsch glacier [Jouvet et al., 2020]. This will make it possible to map the age of the ice. The model used to carry out this work is the Instructed Glacier Model (IGM). This model uses a neural network to emulate the movement of ice [Jouvet et al.,]. In addition to the main objective of mapping the age of the ice, another objective of this internship is to test and optimise certain parts of IGM that are needed to model the age of the ice. Indeed, some tools have been implemented very recently and have not been tested.

3 Data used

The data used in this study have been obtained as follows. In 2020, a field campaign was carried out on the Aletsch glacier to collect ice samples in the area where radionuclides were expected to be found. The sampling positions are shown in figure 3. These samples were analysed at the Spiez laboratory (Federal Institute for Nuclear, Biological and Chemical Protection) to measure the activities of several radionuclides emitted during the Cold War. The protocol for obtaining the data is exactly the same as described in [Jouvet et al., 2020]. Knowing approximately how many nuclear tests were carried out each year during the Cold War, we expect a specific pattern with two peaks in the activity measurements. The earliest peak corresponds to the maximum radionuclide contamination in 1953, the minimum between the two peaks corresponds to 1960 and the second peak corresponds to 1963, when the USA and the USSR signed the Partial Test Ban Treaty [Gabrieli et al., 2011].

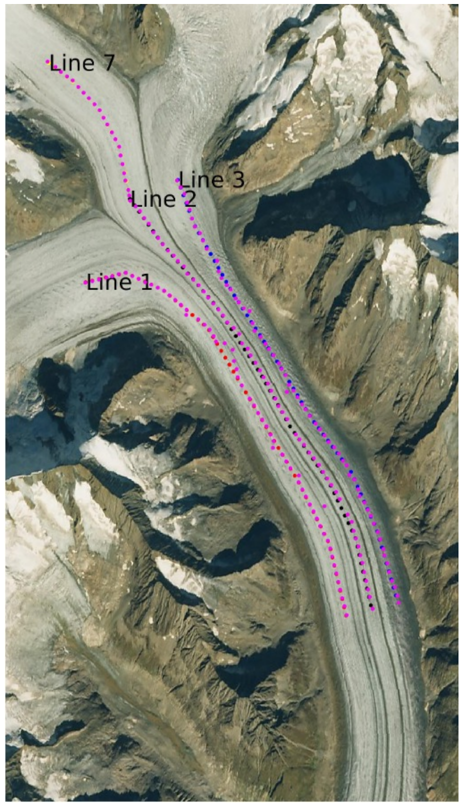

Figure 3: Sampling positions on the glacier. Figure by G. Jouvet

We found that of all the radionuclides measured, ^{236}U, ^{240}Pu and ^{239}Pu had the clearest two-peak pattern. Their activities are shown in figure 4. Knowing that the older the ice, the lower it is in the glacier, we can identify the peaks, and therefore obtain a measure of the position of the 1960 isochronous line on the glacier with an accuracy of the order of a few hundred metres.

We also use digital elevation models (DEMs) of the Aletsch glacier for the years 1880, 1926, 1957, 1980, 1999, 2009 and 2017. DEMs are 3D graphical representations of ground elevation. They are obtained from satellite measurements or, in the case of the oldest DEMs, reconstructed from photographs. Given the topography of the bedrock under the Aletsch glacier, we can deduce the thickness of the glacier by subtracting the bedrock elevation from the DEM. The last piece of data is the meteorological record available for Aletsch glacier since 1880 that allows us to compute the SMB. Except the radionuclides, all the data used in this study are the same as in [Jouvet et al., 2011].

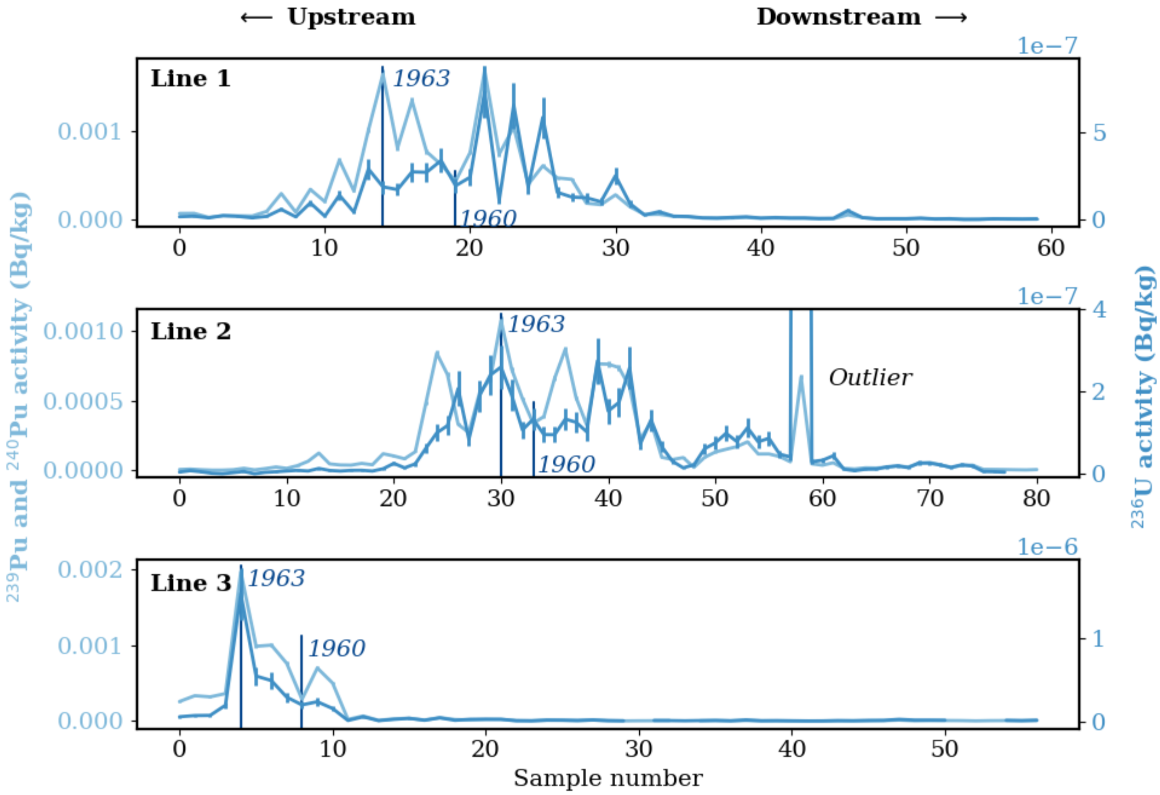

Figure 4: Activities of ^{239}Pu and ^{236}U along the three sample lines defined in figure 3 from upstream to downstream.

4 Model used

Numerical modelling of glaciers is based on following principle. Given the state of a glacier, described by the elevation of its bedrock and the ice thickness at a certain time t_i, and the evolution of the climate over a period running from t_i to t_f, we want to calculate the state of the glacier at time t_f.

From the initial state of the glacier, we calculate the velocity field of the glacier by solving the Stokes equation. This velocity field is used to calculate the deformation of the glacier over a time step dt, which gives the glacier a new shape. Next, the climate forcing is taken into account by raising or lowering the surface of the glacier by the value corresponding to the SMB. This gives us the state of the glacier at time $t + dt$. By iterating this process over time, we can calculate the glacier's movement up to time t_f.

4.1 Main parameters and elements of IGM simulation

The main elements of the numerical simulation used in this study are the calculation of the ice velocity, the calculation of the SMB and the update of the ice thickness. The ice velocity is calculated using a physically informed neural network instead of a finite element method. This is a neural network that takes into account a physical equation in order to constrain the space of admissible solutions. The equation solved by IGM is a high-order approximation of the Stokes equation called the Blatter-Pattyn approximation.

The SMB is calculated using two different methods, depending on the availability of meteorological data. If meteorological data are available, they are used to calculate the amount of ablation or accumulation directly. These data consist of temperature and precipitation measurements taken at a weather station located near Aletsch glacier. Given that Aletsch glacier is around 20 km long, with an altitude varying from 1 700 to 4 000 m, the weather conditions are not constant over the surface of the glacier. They are therefore extrapolated using altitude gradients. If no meteorological data is available, values are entered for the ELA and for the accumulation and ablation gradients, which correspond to the evolution of the glacier extent suggested by the historical and geomorphological data. The amount of accumulation or ablation is calculated from these gradients.

From the velocity field and the SMB, and by solving the conservation of mass equation, we calculate the deformation of the glacier and therefore the new ice thickness.

These elements are used to create a glacier model that reproduces the past dynamics of Aletsch glacier. In addition, there are three post-processing functions, which do not modify the ice dynamics but are used to calibrate the model.

Firstly, whenever a DEM is available (see section 3), the difference between the ice thickness calculated by IGM and the one given by the DEM is calculated. Secondly, as the neural network does not solve the Stokes equation itself but the Blatter-Pattyn approximation, it only calculates u and v, the horizontal components of the velocity. The vertical component of the velocity w is calculated a posteriori by a third post-processing function using the ice incompressibility condition $\overrightarrow{\nabla}.\overrightarrow{u} = 0$. Finally, to calculate the radionuclide trajectory and model the age of the ice, a particle tracking method is used. The particles are initialized on the surface of the glacier in the accumulation zone with a uniform density. Their position is updated at each time step, using the three components of the velocity field [Jouvet et al.,].

4.2 Integrating particles in the simulation

The IGM particle integration method was recently developed and needed to be tested and corrected before being used for age modelling. Two different methods were developed. A series of tests were carried out to check that the behaviour of the particles was consistent from a physical point of view.

The first method, known as ‘simple’, neglects the compression or vertical expansion of the ice and only takes into account the effect of the SMB. This method appears to be a good first-order approximation of particle motion, requiring very low computational cost and producing very smooth results.

The second method, known as 'kinematic', involves integrating the incompressibility condition of the ice $\overrightarrow{\nabla}.\overrightarrow{u} = 0$. This is essentially a mathematical rewrite that requires no additional physical assumptions.

$$w(z) = \frac{\partial z}{\partial x}u + \frac{\partial z}{\partial y}v - \frac{\partial}{\partial x}\left(\int_b^z u\,dz\right) - \frac{\partial}{\partial y}\left(\int_b^z v\,dz\right) \quad (1)$$

The proof of this formula and more informations about particle tracking are presented in the appendices. This method requires slightly longer numerical calculations but produces results that are physically consistent, as shown in Figure 5. In fact, in the synthetic case, we can see the particle that starts its trajectory at the top of the glacier and dive until it almost reaches the bedrock, which does not happen with the 'simple' method. In the following, all the simulations use the 'kinematic' method.

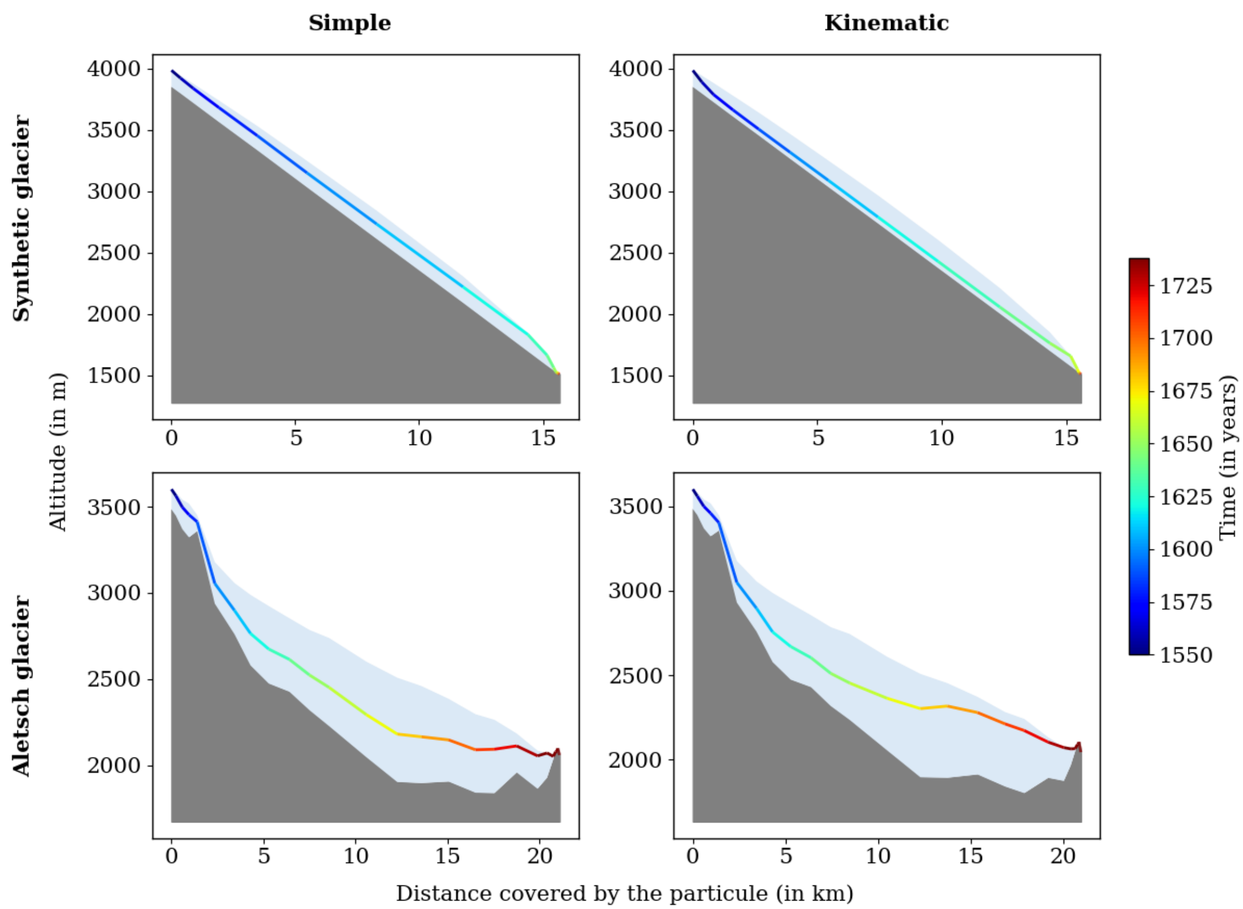

Figure 5: Vertical section of a synthetic glacier and the Aletsch glacier along the trajectory of a particle integrated using the two methods available in IGM.

5 Results

To calibrate all the parameters of the numerical model, the simulation are compared with the data, which covers the period from 1880 to 2020. We are therefore using a simulation of the Aletsch glacier covering this period to calibrate the model. However, we expect that a significant proportion of the ice is older than this, so the simulation must start earlier, despite the lack of meteorological data. To compensate this lack of data, climatological results are used: before the current global warming, there were two different climatic periods in Europe, known as the Medieval Warm Period (from 950 to 1300) and the Little Ice Age (from 1700 to 1850). Geomorphological and historical data relating to these periods allow us to reconstruct the extent of the ice over the past centuries as follows. The Aletsch glacier reached its maximum extent around 1850, which corresponds to the date of the first scientific measurements and left visible clues in the landscape, such as the moraines. Prior to this, it underwent several phases of expansion and retreat [Grove and Switsur, 1994]. Given this information, the modelling strategy for the Aletsch glacier will be carried out in two stages. First, using the data available from 1880 to 2020, calibrate a model over this period. Then, by using the output of this model as input for an extrapolated model starting in 1000 and ending in 2020. This implies the assumption that the state of Aletsch glacier at the time of the medieval climatic optimum and at the present time are similar.

5.1 Model calibration based on radionuclide data

There are many physical parameters that determine the flow of glaciers, which are more or less well known and likely to vary depending on the studied glacier. In our case, the key parameters to be adjusted are the SMB, the viscosity of the ice and the basal sliding, i.e. the boundary condition on the velocity at the base of the glacier, which is not zero for mountain glaciers. For Aletsch glacier, meteorological data is available from 1880 to the present day, so we can describe the SMB in terms of the accumulation and ablation of ice on the surface, which are directly linked to precipitation and temperature. Snowfall corresponds to ice accumulation, modulated by the snow-ice compaction factor. A positive temperature corresponds to melting: annual ablation is therefore proportional to the number of days when the temperature is positive. The meteorological data comes from a station located close to the glacier. However, as the glacier is approximately 20 kilo m long, with an altitude varying from 1 700 to 4 000 m, weather conditions are not constant at the glacier's surface. They are therefore extrapolated with altitude gradients. For temperature, this approximation is correct, but for precipitation, it is not completely satisfaying, given that the topography has a strong influence on precipitation, by trapping clouds for example. This is why we need to correct the precipitation field, using 4 parameters: a global multiplicative factor that applies to the whole glacier, and 3 local multiplicative factors that control accumulation separately for each three basins.

The viscosity of ice depends on its temperature and, for temperate ice, i.e. at melting temperature, on its liquid water content. This is difficult to model, so we simply assume a homogeneous viscosity throughout the glacier, which we adjust by a multiplication factor.

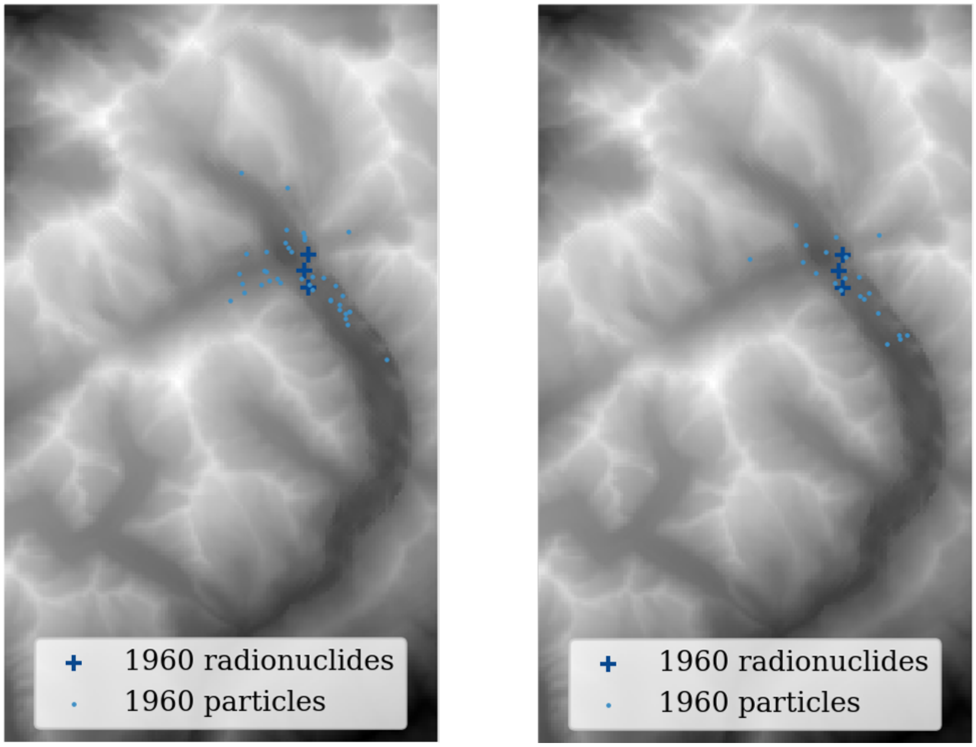

(a) Glissement moyen (b) Glissement faible

Figure 6: Positions of measured surface radionuclides and particles simulating these radionuclides.

Basal sliding depends on topography, bedrock roughness and subglacial hydrology, among other factors. There is very little data available on this subject for Alpine glaciers because it is a very difficult phenomenon to observe since it is physically difficult to access the underside of a glacier. For this reason, we tested two different configurations in order to analyse the sensitivity of this parameter to age modelling. In the first configuration, the ratio between the velocity due to basal sliding and that due to ice deformation is low. In the second configuration, the two speeds are comparable. In the following, we will refer to these configurations as 'low sliding' and 'medium sliding'. They are the two physically consistent limit cases for mountain glaciers.

To ensure that the model is physically realistic, we have two parameters that constrain it: the DEMs, that give us the thickness of the glacier at certain dates, and the radionuclide data, which give us the position of the surface ice dating back to 1960. During the simulations, we measure the difference between these data and the simulation and try to find the parameter values that minimise the two constraints.

To adjust the position of the contaminated ice, we display on a map the position of the radionuclides measured and simulated in 2020 (see Figure 6), in order to visualise the distance between them, which must be as small as possible, despite the dispersion of the particles included in the simulation.

To adjust the ice thickness, we measure the mean difference and standard deviation between the measured and modelled values each time a DEM is available and try to minimise the difference. The mean difference should tend towards zero and the standard deviation should be as small as possible, even though it cannot reach zero. In practice, the smallest standard deviation that can be achieved with IGM for a mountain glacier is between 20 and 30 metres. The values obtained after calibration are presented in table 1.

Medium sliding		
Year	Mean error	Std. dev.
1880	0,00 m	0,00 m
1926	2,80 m	22,16 m
1957	7,82 m	27,29 m
1980	2,02 m	28,18 m
1999	8,58 m	31,10 m
2009	−0,06 m	25,92 m
2017	−5,25 m	25,39 m

Low sliding		
Year	Mean error	Std. dev.
1880	0,00 m	0,00 m
1926	2,4 m	27,51 m
1957	6,68 m	30,91 m
1980	1,23 m	29,67 m
1999	8,65 m	31,87 m
2009	0,66 m	26,07 m
2017	−3,99 m	24,71 m

Table 1: Mean difference and standard deviation between the DEM and the model for ice volume in medium and low sliding configuration.

5.2 Long term run

In order to integrate particles so as to know the age of all the ice currently present in the Aletsch glacier, we need to start the simulation well before 1880. Since no meteorological data is available before this date, we have to describe the SMB in an other way. The solution adopted is to give the values of the accumulation and ablation gradients and the ELA directly as a function of time, in order to reproduce the expected variation in the ice extent from 1000. A large glacier such as the Aletsch has a long response time, which is why the minimum value of the ELA and the maximum of the ice extent are separated in time. It is also important to give enough points to define the ELA in order to avoid large discontinuities that would cause the glacier model to behave unrealistically. The ELA curve used here is shown in Figure 7. The fluctuations in ice extent prior to 1880 are neglected by assuming that the Aletsch glacier only underwent a long phase of retreat during this period. This is equivalent to assuming that the further back in time we go, the less influence the ice extent has on the current age of the ice. In fact, the oldest ice currently found at the bottom of the Aletsch glacier was at the top of the glacier in the past, and is therefore only slightly influenced by the state of the bottom of the glacier at that time.

With this model, we carried out simulations from 1000 to 2020 in medium and low basal sliding configurations, adding new particles initiated in the accumulation zone every 20 years. In the medium sliding configuration, the oldest particles present in the glacier at the end of the simulation began their trajectory in 1480. This suggests that the oldest ice in the

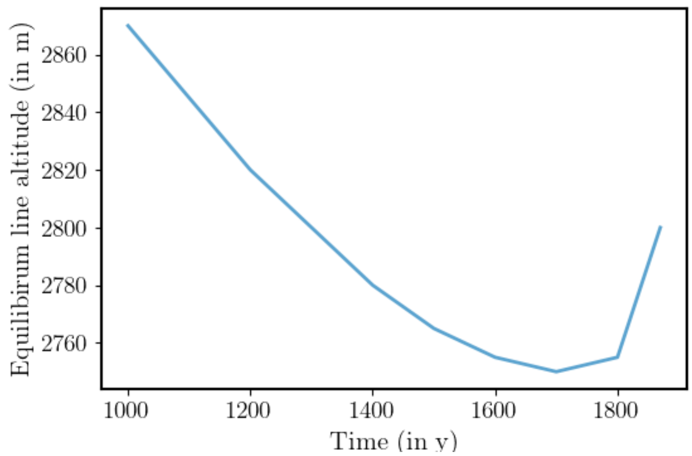

Figure 7: Evolution over time of the ELA used to simulate the Aletsch glacier before 1880

Aletsch glacier, according to the medium simulation, dates from around 1500. In the low-sliding configuration, around twenty of the particles that were seeded in 1000 remain in the glacier. Given that 6037 particles were seeded at that date, we can conclude that, according to the low-sliding simulation, almost all the ice dating from 1000 has now disappeared from the Aletsch glacier, and that the oldest ice in the glacier dates from around 1000. Basal sliding is therefore a parameter that strongly influences the date of the oldest ice currently present in the glacier.

5.3 Mapping the age of ice

To obtain a complete model of the age of the ice, it is necessary to extrapolate the particle data. The Lagrangian model used in this study only gives the age of the ice at the position of each particle. We used a linear interpolation algorithm to obtain the age of the ice at any point on the glacier.

This interpolation gives us a three-dimensional scalar field. To visualise it correctly, there are 3D visualisation tools such as matplotlib, but it is also necessary to visualise the data in two dimensions in order to communicate them easily. Figure 8 shows the age of the ice at the surface of the glacier and at its base in the low and medium sliding configurations. There is virtually no difference between the two models at the surface. However, at the base of the glacier, the low sliding simulation predicts much older ice, which is consistent with the fact that if the ice flows slower, it stays longer in the glacier. It is also consistent to observe very similar results between the two models at the surface, given that the radionuclide data used to calibrate the models comes from samples taken at the glacier surface. We have actually adjusted the parameters of the two models in order to obtain the same position for the surface ice dating from 1960.

It is also interesting to know the vertical distribution of the age. This allows us to visualise

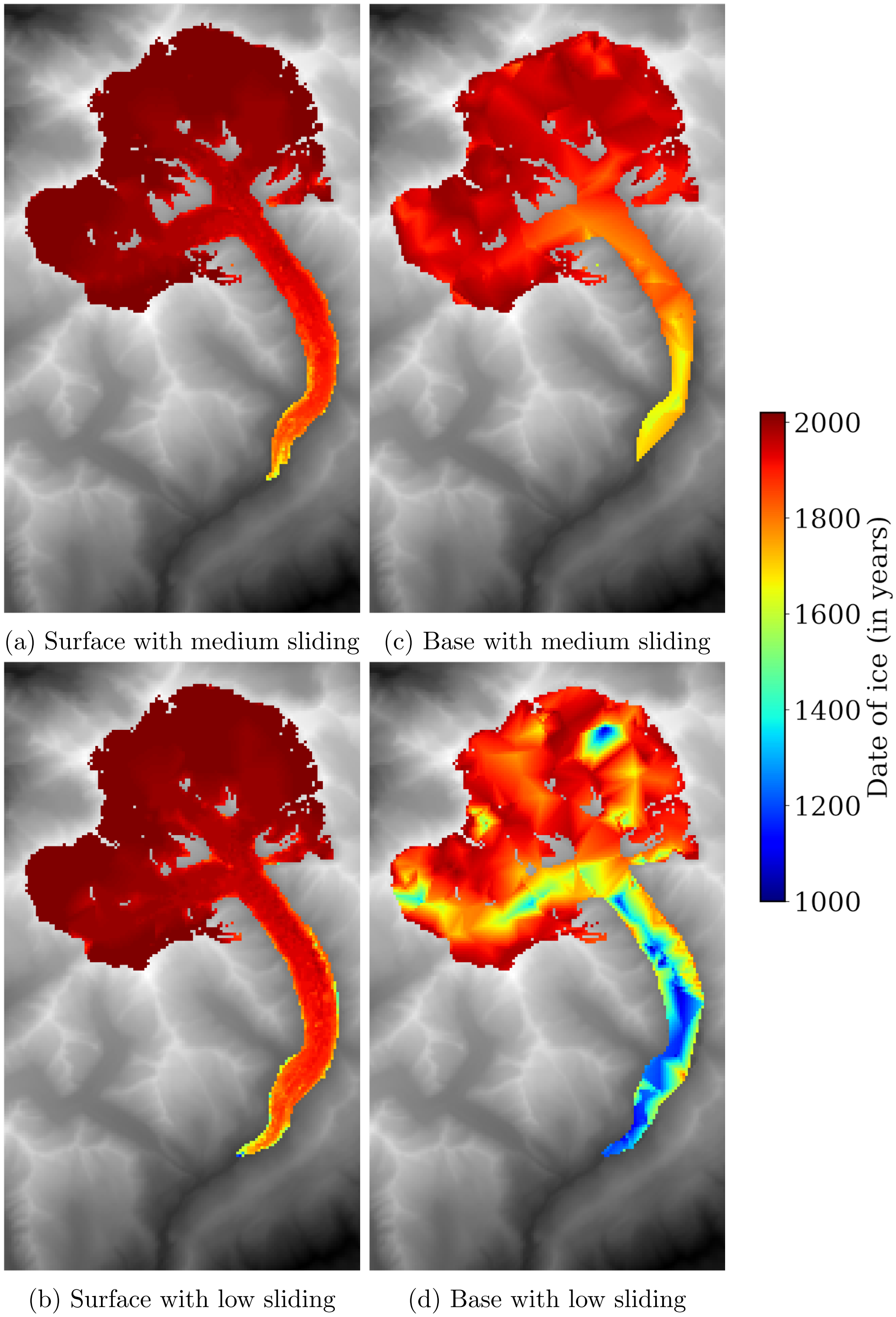

Figure 8: Comparison of the age of the ice in the two basal sliding configurations at the surface of the glacier and at its base. There is no significant difference in the age of the surface ice between the two models, but with low basal sliding, the ice at the base of the glacier is about 500 years older than with medium basal sliding.

the inside of the glacier, and see the amount of young ice compared with the amount of older ice. To access this data, we make vertical sections of the glacier along the flow lines, which are given by the particles trajectories. Figure 9 shows the vertical sections for the two sliding configurations along two almost identical trajectories. Whatever trajectory is chosen, the cross-sections are very similar. That the older the ice, the deeper it is in the glacier and the longer trajectory it goes. The difference between a low and a medium sliding mainly affects the base of the glacier, but not the top or the surface of the glacier. We can also see that in both cases, most of the ice in the glacier is young compared with the maximum age observed against the bedrock. When it is far from the bedrock, the ice is no older than 1700 or 1800.

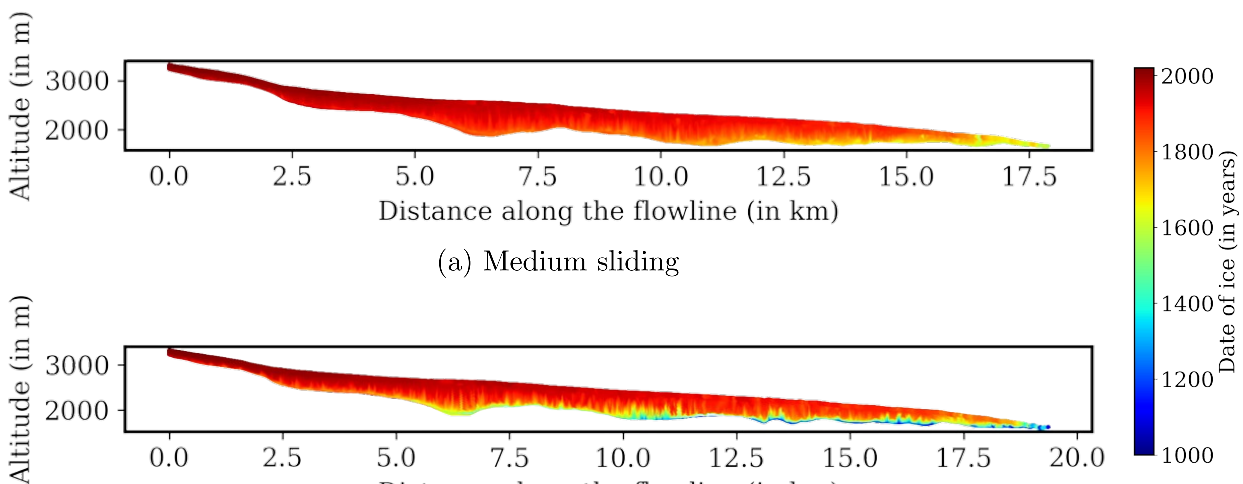

(a) Medium sliding

(b) Low sliding

Figure 9: Vertical sections of the glacier along a flow line as a function of the age of the ice representation

6 Conclusion

Using radionuclide data, a numerical ice flow model and particle tracking, I modelled the age of the ice in the Aletsch glacier. This is the first time that such a mapping, particularly the vertical section, has been carried out for a mountain glacier. According to the models, most ice dates from between the 18th century and present time. However, there is much older ice near the bedrock. Depending on the basal sliding, which is not well known, the oldest ice could date from between 1000 and 1500. The basal sliding has a negligible influence on the result of the modelling for the glacier surface, but it would be interesting to have more data to constrain the age value along the bedrock with more precision.

I studied the particle tracking method in IGM and made some corrections and optimisations in it. The current 'kinematic' and 'incompressibility' methods give consistent results, but the error between them remains non negligible.

This particle-tracking method has many possible applications, particularly in modelling the transport of clasts within glaciers. I have therefore collaborated with Léa Rodari, another Master student of the ICE group who is studying englacially transported clasts in the Mer de Glace, and I will be using my model of the Aletsch glacier to produce results for Katarina Wetterauer, a PhD student at the Deutsches GeoForschungsZentrum (German Earth Sciences Research Centre) in Potsdam.

It would also be interesting to extend this study to other glaciers in the Alps. Studying the age of the ice in mountain glaciers opens up the possibility of studying the climate archives they contain. In particular, this would make it possible to compare with data from the polar ice caps, which are already well documented, to gain a better understanding of local climatic variations over the last few centuries.

Acknowledgments

I would like to thank Guillaume Jouvet, who guided me during this internship. He taught me a lot about glacial processes and numerical modelling, but also about scientific writing and communication. It was always a pleasure to talk and work with him, and to share his enthusiasm for research.

I would also like to thank the entire ICE group for their very warm welcome to Unil. Special thanks to Léa Rodari, who was a pleasure to work with and helped me to proofread my report, and to Brandon Finley and Kejdi Lleshi, who shared their office with me.

Thanks also to Martin Thiriet, who gave me the idea and the equations for an analytical velocity field that helped me to adress the problem of the vertical velocity with more rigour.

Summary calendar

- **2 April - 15 April**: Bibliographical research, familiarisation with IGM through basic simulations, analysis of field data.
- **15 April - 1 May**: First calibration of the parameters of the Aletsch glacier using the simple particle tracking method.
- **1 May - 27 May**: Tests and corrections on the particle tracking module. Study of the vertical velocity.
- **27 May - 12 June** : Readjustment of the calibration of the parameters of the Aletsch glacier using the kinematic method, integration of the particles into a long-term simulation and interpolation of the results to create the age map.
- **13 June - 28 June**: Writing the report and preparation of oral presentations for the ICE group and for the internship defense. Developping the code to use particles data to model englacially transported clasts with Léa Rodari.

- **1 July - 26 July** : Optimisation and correction of the kinematic method to compute the vertical velocity, development of the analytical test and correction of the incompressibility method.

References

[Gabrieli et al., 2011] Gabrieli, J., Cozzi, G., Vallelonga, P., Schwikowski, M., Sigl, M., Eickenberg, J., Wacker, L., Boutron, C., Gäggeler, H., Cescon, P., et al. (2011). Contamination of alpine snow and ice at colle gnifetti, swiss/italian alps, from nuclear weapons tests. *Atmospheric environment*, 45(3):587–593.

[Glen, 1953] Glen, J. W. (1953). Rate of Flow of Polycrystalline Ice. *Nature*, 172:721–722.

[Grove and Switsur, 1994] Grove, J. M. and Switsur, R. (1994). Glacial geological evidence for the medieval warm period. *Climatic Change*, 26(2):143–169.

[Jouvet and Cordonnier, 2023] Jouvet, G. and Cordonnier, G. (2023). Ice-flow model emulator based on physics-informed deep learning. *Journal of Glaciology*, pages 1–15.

[Jouvet et al.,] Jouvet, G. et al. Concepts and capabilities of the instructed glacier model (igm v2.2.1). https://doi.org/10.31223/X5T99C.

[Jouvet et al., 2020] Jouvet, G. et al. (2020). Mapping the age of ice of gauligletscher combining surface radionuclide contamination and ice flow modeling. *The Cryosphere*, 14(11):4233–4251.

[Jouvet et al., 2011] Jouvet, G., Huss, M., Funk, M., and Blatter, H. (2011). Modelling the retreat of grosser aletschgletscher, switzerland, in a changing climate. *Journal of Glaciology*, 57(206):1033–1045.

[Marzeion et al., 2018] Marzeion, B., Kaser, G., Maussion, F., and Champollion, N. (2018). Limited influence of climate change mitigation on short-term glacier mass loss. *Nature Climate Change*, 8(4):305–308.

7 Appendices

7.1 IGM setups and codes used

7.1.1 IGM setups

These are the main setups that have been used for this work.

- `aletsch_opti` : This is a dynamic simulation of Aletsch glacier from 1880 to 2020, used to find parameters that reproduces the best the past evolution of the glacier. It uses an input produced with the `optimize` module, and a SMB computed from weather data. It has two possible configurations, with a low or medium basal sliding.
- `aletsch_past` : This is a dynamic simulation of Aletsch glacier from 1000 (or 500) to 2020, with the parameters found using the previous calibration setup. It has been used to integrate particles in the simulation in order to track the age of ice. It has two possible configurations, with a low or medium basal sliding.
- `synthetic` : This allows to create a synthetic glacier on a bed that has the shape of a parabola. Using constant SMB and running the simulation during a very long time, it tends towarads a stationnary state. The output is used as an input for the next stationnary simulation.
- `synthetic_stationnary` : Using the output from the previous simulation as an input, this is a stationnary synthetic glacier that has been used to observe the vertical velocity and particles motion, and check that IGM porduces a realistic behaviour.
- `analytical_case` : In order to check that the vertical velocity w computed by IGM is accurates, this setup assigns values to u and v that correspond to a velocity field that is analyticaly known, so that we can compare the w field computed by IGM with the theoretical one.

The setup used in `aletsch_opti` simulation is the following. I slightly modified the modules `time` and `particles`. It allowed me to seed particles in 1960 only, and to compare the model with the DEMs each time it is possible without saving a huge amount of data at each simulation. I also wrote a `plot2d_isochrone` module which is inspired from the `plot2d` module but selects the particles forming isochrone lines on surface of the glacier. That means the particles that have been on the surface of the glacier since less than two years. It allowed me to compare the particles seeded in 1960 with the radionuclides. The particles integrated in IGM, such as solid debris, stay on surface of the glacier once they emerged from it. Radionuclides does not behave this way : they are leached out by melting water so that they don't remain on the surface of the glacier. This is why we only observe radionuclides on an isochrone line and not on an entire surface.

Listing 1: Parameters used for the calibration (aletsch opti) in the medium sliding optimised configuration

```json
{
  "modules_preproc":
    ["load_ncdf","track_usurf_obs"],
  "modules_process":
    ["clim_aletsch","smb_accmelt","iceflow","vert_flow","time_tuning","thk",
     "particles_CM"],
  "modules_postproc":
    ["write_ncdf","plot2d_isochrone","print_info","print_comp","write_particles"],
  "lncd_input_file": "geology-optimized-med.nc",
  "time_start": 1880.0,
  "time_end": 2020.0,
  "time_save": 1,
  "plt2d_live": false,
  "weight_Aletschfirn": 1.1,
  "weight_Jungfraufirn": 0.8,
  "weight_Ewigschneefeld": 0.6,
  "weight_ablation": 1.25,
  "weight_accumulation": 1.2,
  "iflo_init_arrhenius": 78,
  "iflo_init_slidingco": 0.0595,
  "iflo_enhancement_factor": 2.6,
  "part_frequency_seeding": 200,
  "part_tracking_method": "3d",
  "part_density_seeding": 1,
  "tlast_seeding_init": 1760,
  "isochrone_csv": true,
  "track_err_csv": true,
  "vflo_method": "kinematic"
}
```

Parameter	Medium sliding model	Low sliding model
Arrhenius factor	78	150
Sliding coefficient	0.0595	0.1
Iceflow enhancement factor	2.6	1.6
Global accumulation weight	1.2	1.2
Ewigschneefeld accumulation weight	0.6	0.6
Aletschfirn accumulation weight	1.1	1.3
Jungfraufirn accumulation weight	0.8	0.8

Table 2: Values of the parameters in both basal sliding configurations after tuning the simulation to minimize the misfit between data and model.

This is the `params.json` file used to perform the `aletsch_past` simulation. I developped or modified some modules compared to the main version of IGM available on github, especially the SMB and plot2d modules. The `double_smb` selects the SMB method depending on the time : before 1880, no weather data are available so the SMB is computed with `smb_simple`, using ELA and gradients. After 1880, the `smb_accmelt` module of the Aletsch-1880-2100 example of IGM is used, that takes in account the weather data. The `plot2d_isochrone` selects the particles that are just emerging on surface of the glacier (particles on surface of the glacier since less than two years), plots them and save them in a csv file. This was useful to compare particles and radionuclides positions. For the low and med sliding configurations, the same parameters were used, exept those mentionned in 2.

Listing 2: Parameters used for the long term simulation (aletsch past) with medium basal sliding

```
{
  "modules_preproc":
    ["load_ncdf_custom"],
  "modules_process":
    ["clim_aletsch","double_smb","iceflow","time_tuning","thk","vert_flow",
     "particles"],
  "modules_postproc":
    ["write_ncdf","print_info","print_comp","write_particles","plot2d_isochrone"],

  "smb_simple_array":
    [["time", "gradabl", "gradacc", "ela", "accmax"],
     [ 1000,     0.009,    0.004,  2870,     2.0],
     [ 1200,     0.009,    0.004,  2820,     2.0],
     [ 1400,     0.009,    0.004,  2780,     2.0],
     [ 1500,     0.009,    0.004,  2765,     2.0],
     [ 1600,     0.009,    0.004,  2755,     2.0],
     [ 1700,     0.009,    0.004,  2750,     2.0],
     [ 1800,     0.009,    0.004,  2755,     2.0],
     [ 1870,     0.009,    0.004,  2800,     2.0]],

  "lncd_input_file": "geology-optimized-med.nc",
  "time_start": 1000.0,
  "time_end": 2020.0,
  "time_save": 10.0,
  "iflo_retrain_emulator_nbit_init": 1000,
  "iflo_init_slidingco": 0.0595,
  "weight_Aletschfirn": 1.1,
  "weight_Jungfraufirn": 0.8,
  "weight_Ewigschneefeld": 0.6,
  "weight_ablation": 1.25,
  "iflo_enhancement_factor": 2.6,
  "weight_accumulation": 1.2,
```

```
  "iflo_init_arrhenius": 78,
  "part_frequency_seeding": 20,
  "part_tracking_method": "3d",
  "part_density_seeding": 1,
  "vflo_method": "kinematic",
  "isochrone_csv": true,
  "wncd_vars_to_save":
    ["topg","usurf","thk","smb","velbar_mag","velsurf_mag","uvelsurf","vvelsurf",
     "wvelsurf","icemask"]
}
```

7.1.2 List and description of the IGM modules and codes

IGM modules Here is a brief description of the main IGM modules written for this study.

- `plot2d_isochrone` : Adapted from `plot2d`. Not all the particles are plot on the figure. Only the ones that have come to the surface recently are selected in order to get isochrones. It also plots the position of the 1960 and 1963 measured radionuclides. There is an option to only select the 1960 particles (that is currently activated but can be "switched off" by commenting/uncommenting some lines in the code). It is also possible to add the plot of a 2d field such as `thk` or `velbar_mag` by setting `plt2d` parameter to true.

- `iceflow_analytic` : Assigns values to `state.U`, `state.V` and `state.Wanalytic` using several possible analytical expressions for the velocity field (expressions given by Martin Thiriet). This module must be used with `make_analytic` that defines the grid, topography and ice thickness of the analytical "glacier", and `time_analytic`.

- `make_analytic` : Defines the grid, topography and ice thickness of the analytical "glacier". There are several topographies possible. This module must be used with `make_analytic` that assigns values to `state.U`, `state.V` and `state.Wanalytic` using several possible analytical expressions for the velocity field, and with `time_analytic`.

- `time_analytic` : This module is necessary to use `iceflow_analytic` and `make_analytic` (analytical velocity field). The part with `state.dt_target` is removed (non necessary for the analytical case that is stationnary) beacause it requires variables that are not calculated with the analytical field (`ubar` and `vbar`).

- `vert_flow_analytic` : This is `vertflow` but computes w using both kinematic and incompressibility methods, and compares them to the analytical w. The kinematic method gives exactly the same result as the standard IGM version, the incompressibility method has a different boundray condition, to respect the analytical field that does not satisfy the bedrock impermeability condition when the topography is not flat.

- `particles_test` : Personnal version of the `particles` module. There is an option to seed particles at points given at specific coordinates. There is an other option, made to be used with the synthetic glacier, to seed only 4 particles on the medium line. This is used to produce the vertical cuts. The code line that updates the x position of the particle is commented, so the particles move along a line.
- `plot_final_traj` : Adapted from `plot2d`. Given a particle ID (or a list of IDs), it saves its position at each iteration in a state variable and plots it in the end of the run.
- `vert_flow` : Computes the vertical velocity with two possible methods. Details about this module are given further in the appendix.

Other codes These codes are written to study the data produced by IGM.

- `scipy_3d_interp` : This code contains a list of functions that carry following tasks. Input data is the output file and the positions and ages of all the particles present in the glacier at the end of a simulation (used with `aletsch_past`). It creates interpolation function for the age of particles, to get the age of ice at any position in the glacier, and not only at the particles positions. It makes several possible plots, especially vertical cuts of the age of ice, and 2D maps of the age of ice at given depth in the glacier.
- `vert_cut` : Shows a vertical cut of a glacier along the trajectory of a particle (bedrock and ice surface), and the trajectory of this particle within the glacier.
- `plot_trajectories` (written with Léa Rodari and Guillaume Jouvet) : Select one or several particles that come close enough to a given point in the glacier and saves their trajectories in dedicated csv file. Plots the trajectories on a 2D maps and make vertical cuts of the glacier along one of the selected trajectories. This is useful to study clasts transportation.

7.2 Particle tracking and vertical velocity

7.2.1 Particle tracking formulas

Notations and hypothesis To simplify, we consider a two-dimensional situation. We consider a particule within a glacier, as represented on figure 10. The glacier is defined by a bedrock $b(x)$ and a surface $s(x,t)$. Therefore the thickness of the ice is $h(x,t) = s(x,t) - b(x)$. The particle is described by its Cartesion coordinates $(x(t), z(t))$, and velocity vector $\overrightarrow{u} = u\overrightarrow{e_x} + w\overrightarrow{e_z}$, where $u = \dfrac{\mathrm{d}x}{\mathrm{d}t}$ and $w = \dfrac{\mathrm{d}z}{\mathrm{d}t}$.

We assume that the ice is incompressible, ie

$$\overrightarrow{\nabla}.\overrightarrow{u} = 0, \tag{2}$$

We define the relative height of the particle inside the glacier as $r = \frac{z-b}{h}$.

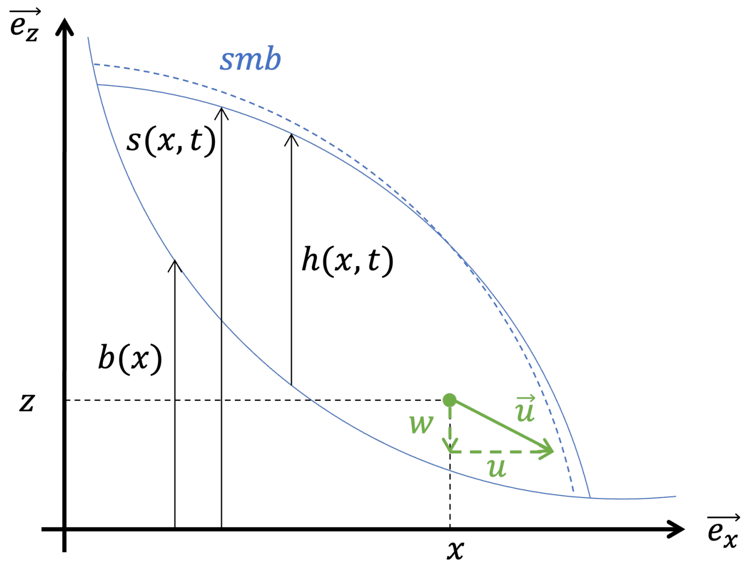

Figure 10: Schematic view of a glacier and notations used in the demonstrations

We assume an impermeability boundary condtion on the bedrock, which implies that the velocity along the bedrock is tangent to it (see fig. 11), gives us following relation :

$$\frac{\mathrm{d}b}{\mathrm{d}x} = \frac{w(x, b(x))}{u(x, b(x))}, \tag{3}$$

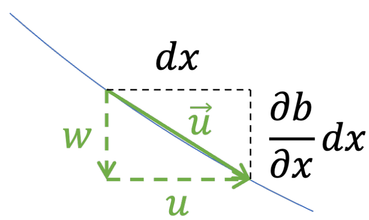

Figure 11: Boundary condition for the velocity along the bedrock

'Incompressibility' formula The first idea is basically to integrate the incompressibility condition in order to get an expression of w as a function of u and v that are computed by IGM iceflow module.

We start with

$$\frac{\partial u}{\partial x} + \frac{\partial w}{\partial z} = 0 \tag{4}$$

Therefore

$$w(z) - w(b) = -\int_b^z \frac{\partial u}{\partial x}\, dz \tag{5}$$

And using the impermeability condition of the bedrock :

$$\boxed{w(x,z) = u(x,b(x))\frac{\partial b}{\partial x} - \int_b^z \frac{\partial u}{\partial x}(x,z)\,dz} \tag{6}$$

Or in 3 dimensions

$$w(x,y,z) = u(x,y,b(x,y))\frac{\partial b}{\partial x} + v(x,y,b(x,y))\frac{\partial b}{\partial y} - \int_b^z \frac{\partial u}{\partial x} + \frac{\partial v}{\partial y}\,dz. \tag{7}$$

'Kinematic' formula This formula is physically the same as the 'incompressibility' one. It is essentially a permutation between integral and derivative using Leibniz rule.

Here is the Leibniz rule

$$\frac{\partial}{\partial x}\left(\int_b^z u\,dz\right) = \frac{\partial z}{\partial x}u(x,z(x)) - \frac{\partial b}{\partial x}u(x,b(x)) + \int_b^z \frac{\partial u}{\partial x}\,dz \tag{8}$$

We recognise the last term of this equation, that is the same as the last term in (6), so we substitute in (6) and get

$$w(x,z) = u(x,b(x))\frac{\partial b}{\partial x} - \frac{\partial}{\partial x}\left(\int_b^z u\,dz\right) + \frac{\partial z}{\partial x}u(x,z(x)) - \frac{\partial b}{\partial x}u(x,b(x)) \tag{9}$$

That we can simplify into

$$\boxed{w(x,z) = \frac{\partial z}{\partial x}u(x,z(x)) - \frac{\partial}{\partial x}\left(\int_b^z u\,dz\right)} \tag{10}$$

Or in 3 dimensions

$$w(x,z) = \frac{\partial z}{\partial x}u(x,y,z) + \frac{\partial z}{\partial y}u(x,y,z) - \frac{\partial}{\partial x}\left(\int_b^z u\,dz\right) - \frac{\partial}{\partial y}\left(\int_b^z v\,dz\right). \tag{11}$$

'Simple' formula We know that the height of the glacier is governed by the following equation, which can be deduced from mass conservation :

$$\frac{\partial h}{\partial t} + \overrightarrow{\nabla}.\overrightarrow{q} = \text{smb}, \tag{12}$$

where

$$\overrightarrow{q} = \int_b^s \overrightarrow{u}\,dz \tag{13}$$

is the flux of the velocity vector across the vertical section of the glacier and smb is the surface mass balance of the glacier, ie the combination of accumulation and ablation of ice on the surface of the glacier.

We define the relative height of the particle inside the glacier as

$$r = \frac{z - b}{h}. \tag{14}$$

According to the definition,

$$w = \frac{\mathrm{d}z}{\mathrm{d}t}. \tag{15}$$

We can express z as a function of r : $z = rh - b$, therefore

$$w = h\frac{\partial r}{\partial t} + r\frac{\partial h}{\partial t}. \tag{16}$$

Using the equation (12), we substitute $\frac{\partial h}{\partial t}$

$$w = h\frac{\partial r}{\partial t} + r\left(\mathrm{smb} - \overrightarrow{\nabla}.\overrightarrow{q}\right). \tag{17}$$

We assume that $w \approx -r\overrightarrow{\nabla}.\overrightarrow{q}$ and we can therefore simplify previous equation.

$$\boxed{\frac{\partial r}{\partial t} = -\frac{r}{h}\,\mathrm{smb}} \tag{18}$$

7.2.2 1st order correction of gradients to consider the slope

Given the vertical discretization of IGM, we can compute gradients along the axis in the base (x, z) that is not orthogonal. z is the vertical axis but x is not horizontal. It follows the local slope of the considered layer. However, to implement the incompressibility formula, we need the gradient in the orthogonal basis (x_0, z_0).

The basis change can be done using following matrix

$$\begin{pmatrix} A_0 \\ B_0 \end{pmatrix} = \begin{pmatrix} \cos\theta & -\sin\theta \\ 0 & 1 \end{pmatrix} \begin{pmatrix} A \\ B \end{pmatrix} \tag{19}$$

Where θ is the local angle between x and x_0. We have $\tan\theta = \frac{\partial z}{\partial x}$, defined as the slope of the layer z. We can also write this

$$\begin{pmatrix} A_0 \\ B_0 \end{pmatrix} = \begin{pmatrix} \frac{1}{\sqrt{\left(\frac{\partial z}{\partial x}\right)^2 + 1}} & -\frac{\frac{\partial z}{\partial x}}{\sqrt{\left(\frac{\partial z}{\partial x}\right)^2 + 1}} \\ 0 & 1 \end{pmatrix} \begin{pmatrix} A \\ B \end{pmatrix} \tag{20}$$

Assuming that the slopes are low, we can use the small angles approximation and therefore the matrix becomes

$$\boxed{\begin{pmatrix} 1 & -\frac{\partial z}{\partial x} \\ 0 & 1 \end{pmatrix}} \tag{21}$$

Finally, we shall use following formula in IGM to compute horizontal derivatives (and same formula with y instead of x) :

$$\boxed{\frac{\partial u}{\partial x_0} = \frac{\partial u}{\partial x} - \frac{\partial z}{\partial x}\frac{\partial u}{\partial z}} \tag{22}$$

Note that this correction only affect the incopressibility method. In the kinematic one, the effect of the slopes is already taken in account in the Leibniz formula.

7.2.3 Analytical velocity field

We use following velocity field that is incompressible.

$$u = v_0, \qquad v = -y\frac{v_1}{H}\left(1 - \frac{2x}{L}\right), \qquad w = z\frac{v_1}{H}\left(1 - \frac{2x}{L}\right)$$

where v_0 and v_1 are constants, L is the lenght of the parallelepipede in the x direction and H is its height (in the z direction).

Both kinematic and incompressibility methods produce very good results, the errors are only a noise due to numerical precision of calculs, that is negligible. For the kinematic method there is an error on the borders of the paralellogram, which is not critical because the grids used in IGM are always larger than the modelled glaciers, which therefore does not get affected by this problem. But, given that the topography is flat, and that u and v are not functions of z, some terms in previous equations are equal to zero, therefore we did not completely tested the two methods, this case is too simple and further tests are necessary.

7.2.4 Results

Figure 12 shows the trajectory of a perticule integrated with each method available in IGM, on the synthetic stationnary glacier and on a dynamic simulation of Aletsch glacier. With each method, we can see that the particle dives in the glacier, but the trajectory if different with each method. Concerning the simple method, this is coherent because the equation implemented neglects part of the physics governing the vertical velocity of ice. Concerning the difference between incompressibility and kinematic, the difference could be only due to the disretization or numerical precision, or resulting of an error in one ore both methods.

To ensure that there is no error in the implementation od kinematic and incompressibility method, a more complex analytical velocity field woud be necessary, but has not be done yet. The influence of the vertical discretization has been tested on the synthetic glacier.

Synthetic glacier Two simulations have been performed with a different vertical discretization. The first one uses the standard discretization with 10 layers and the second one uses a 30 layers vertical discretization. It was not possible to test other configurations because changing the vertical discretization requires to change the emulator and there are pretrained emulators for only 10 and 30 layers. With 10 layers, the error between incomressibility and kinematic method at the point where the vertical velocity is maximal reaches 12%

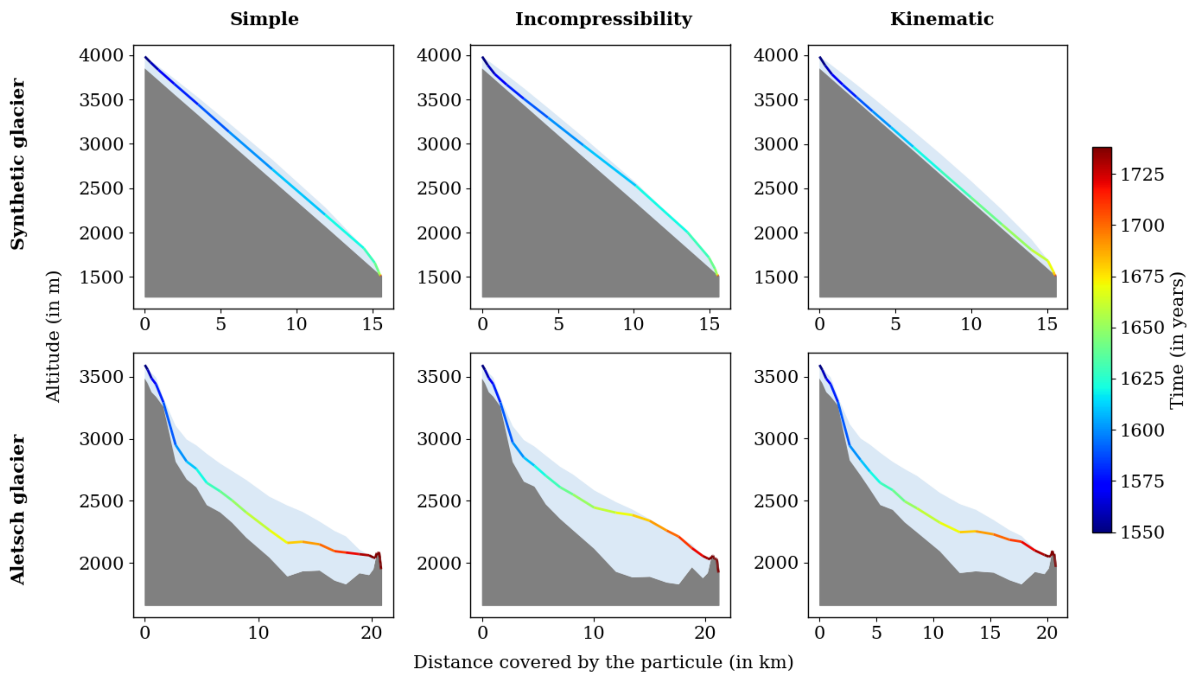

Figure 12: Vertical section of a synthetic glacier and the Aletsch glacier along the trajectory of a particle integrated using the three methods available in IGM.

(see figure 16), and the trajectory of the particle is longer with the kinematic method (see figures 13 and 14). With 30 layers, the error between incomressibility and kinematic method at the point where the vertical velocity is maximal reaches 4% (see figure 16), which is a third of the previous error. Given that we tripled the number of layers, it suggests an inverse dependency between the error and the number of layers. The particles trajectories are also closer to each other with 30 layers, and tends towards something intermediate between the kinematic and incompressibility trajectories with 10 layers (see figures 17 and 18).

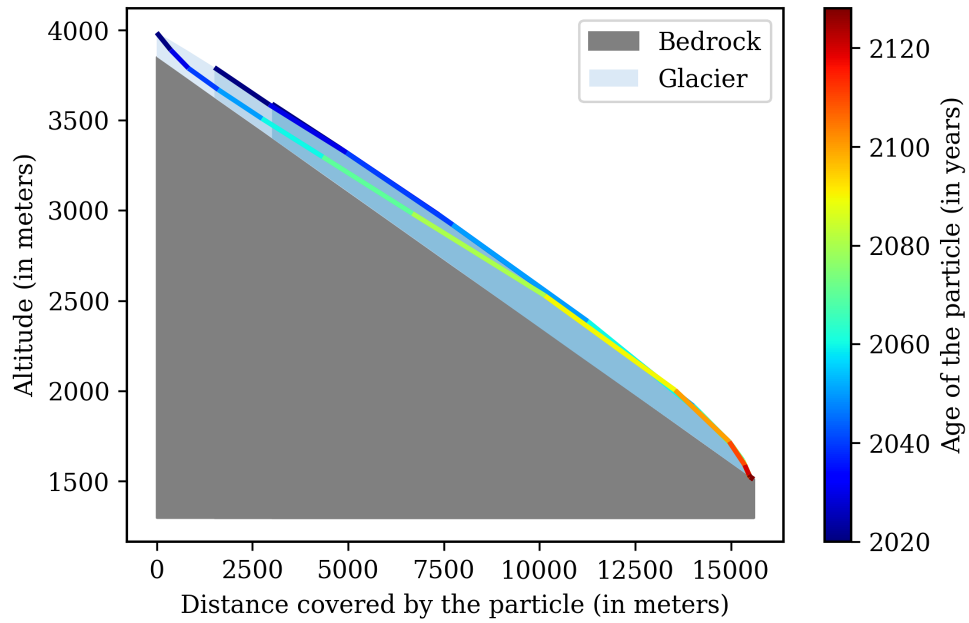

Figure 13: Incompressibility method with 10 layers

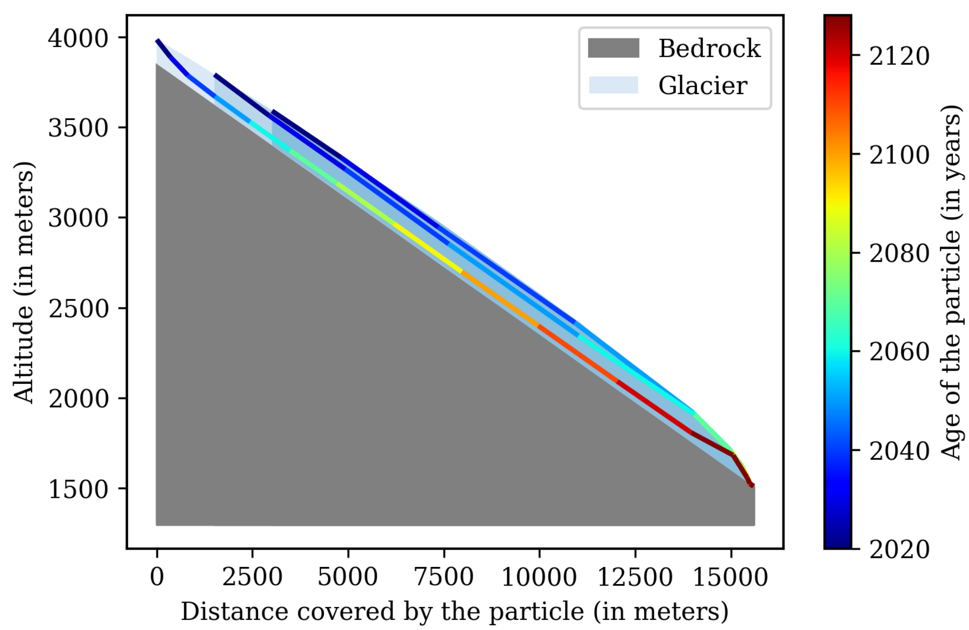

Figure 14: Kinematic method with 10 layers

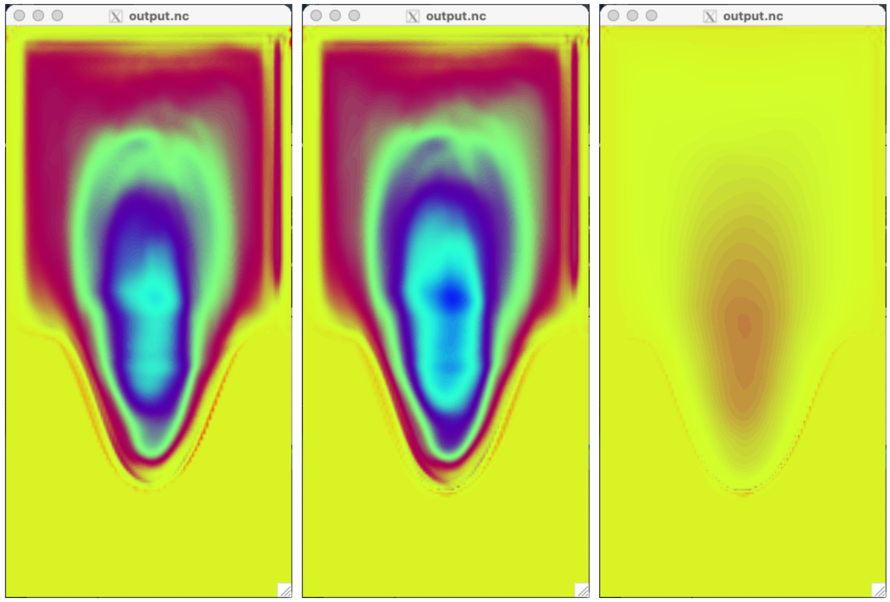

(a) Wi (b) Wk (c) Wk - Wi

Figure 15: W on the surface of the synthetic glacier with 10 layers

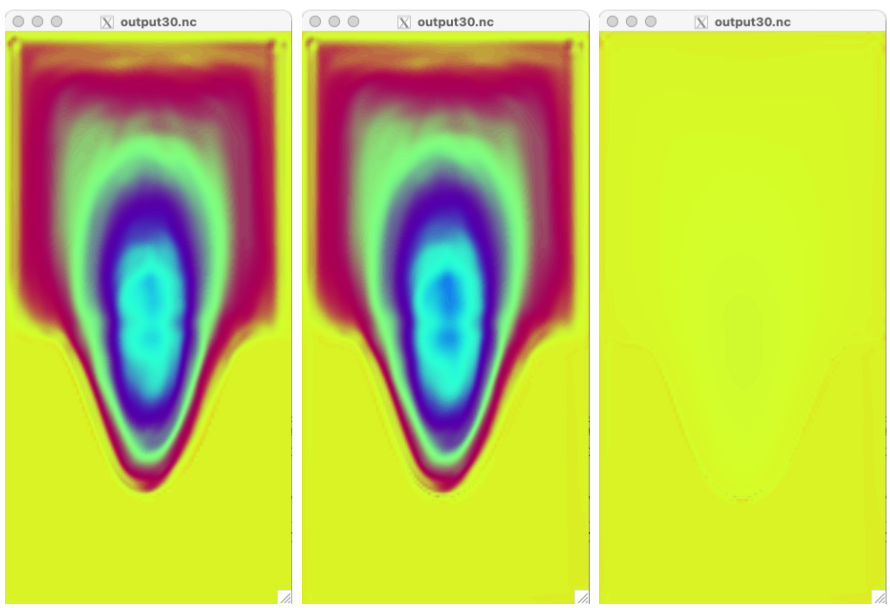

(a) Wi (b) Wk (c) Wk - Wi

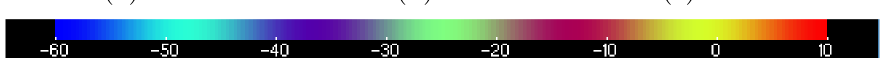

Figure 16: W on the surface of the synthetic glacier with 30 layers

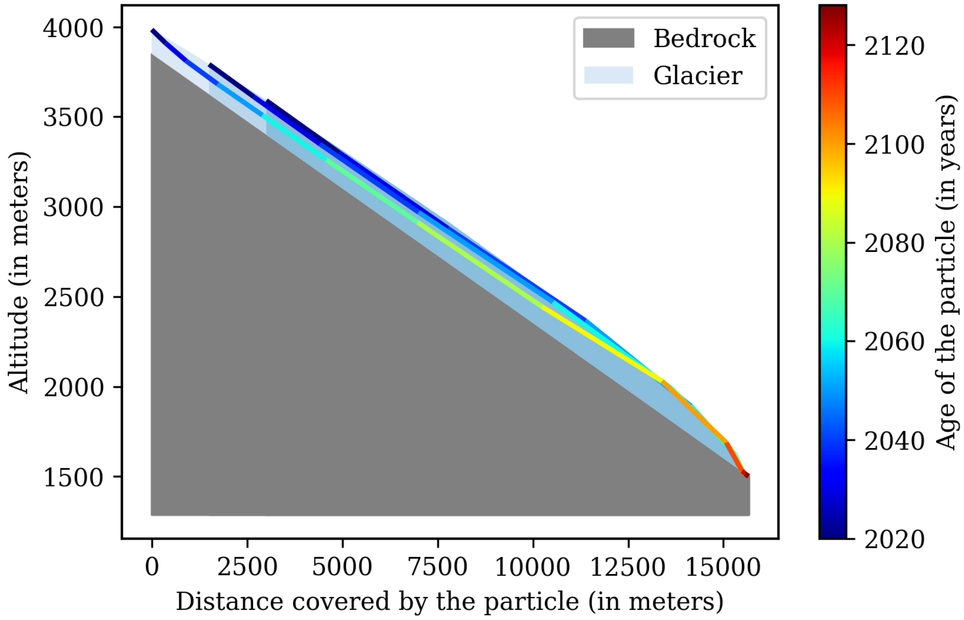

Figure 17: Incompressibility method with 30 layers

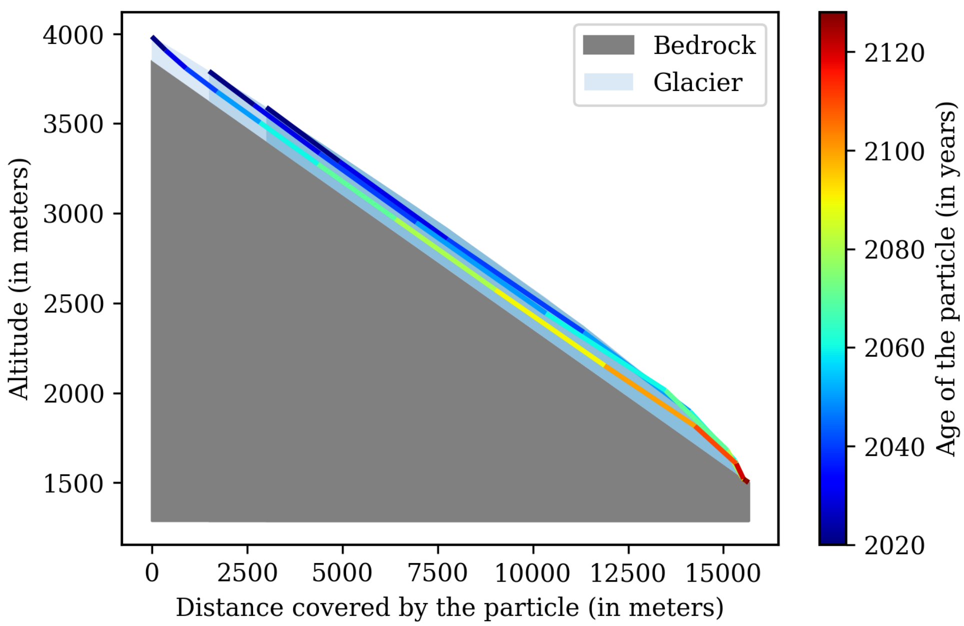

Figure 18: Kinematic method with 30 layers

Aletsch glacier We tested the two methods on Aletsch glacier. They give very similar vertical velocity fields and with an error between them of a few percents. The particles trajectory is shorter with the incompressibility method, exactly as on the synthetic glacier. The result obtained with the kinematic methods seems to be more accurate, but it would be interessant to get evidence about this. There would be three ways to achieve this. The first one would be to find an analytical case more complex, as described in a previous section. The second would be to compare this modelisation result with field data, for example by seeding GPS trackers in the accumulation area of the glacier and recording their trajectories within the glacier. The problem is that it takes about two hundred years, therefore this should be done on a smaller glacier than Aletsch glacier. The last method would be to use an an analog model to perform the same but at a smaller time scale.

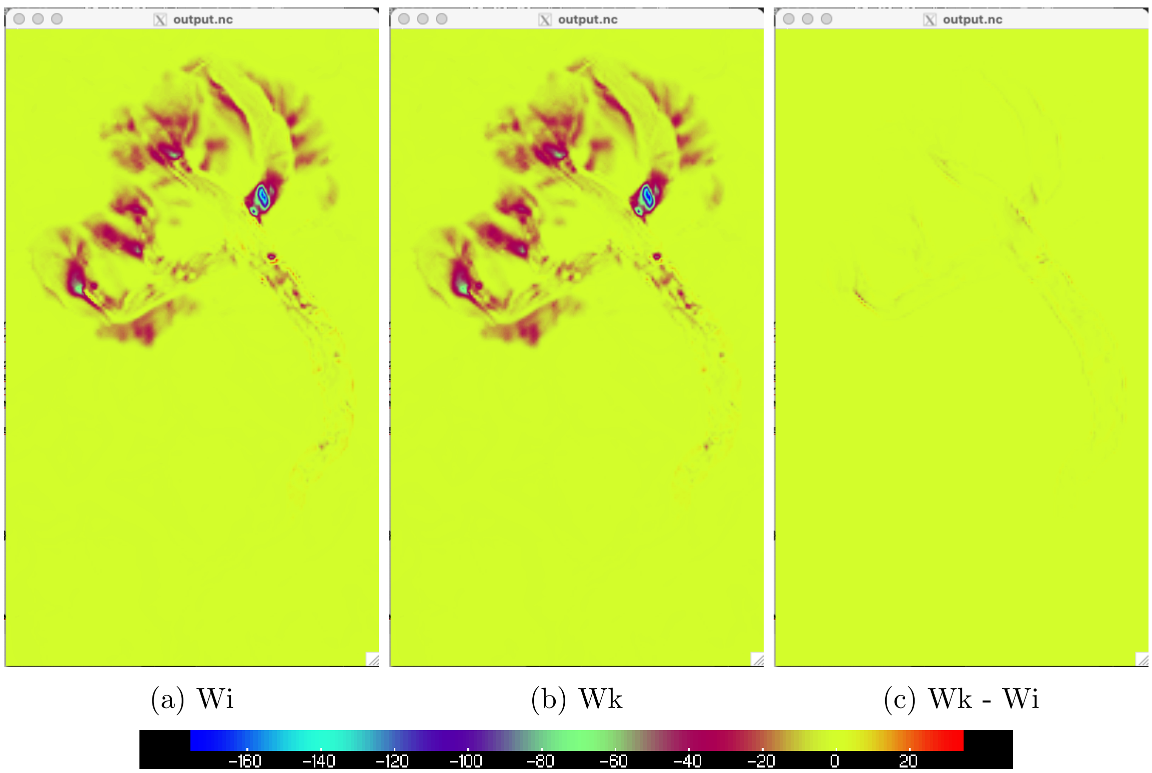

(a) Wi (b) Wk (c) Wk - Wi

Figure 19: W on the surface of Aletsch glacier

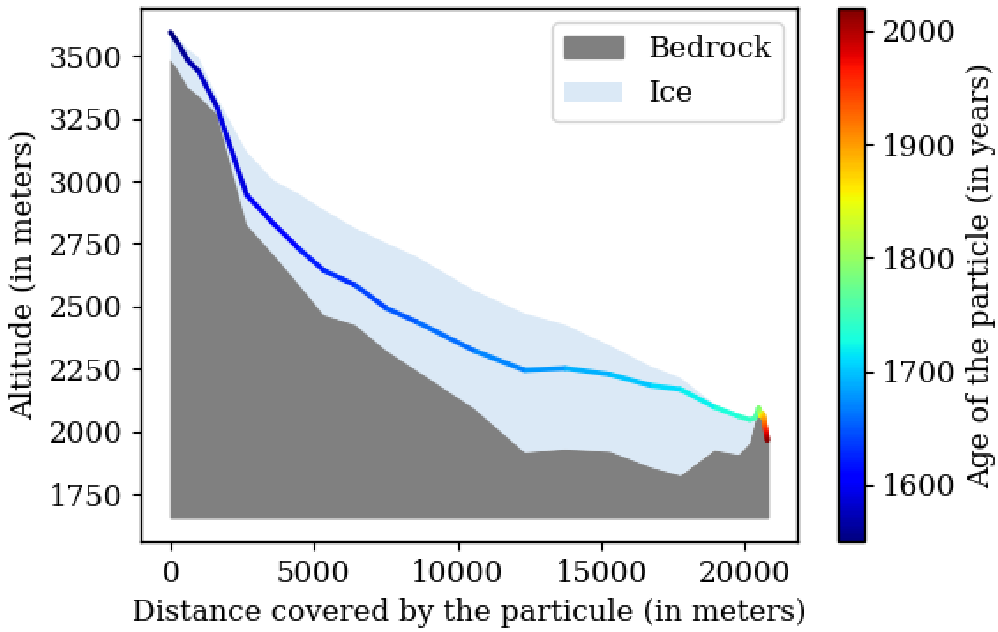

Figure 20: Trajectory of a particle in Aletsch glacier with kinematic method

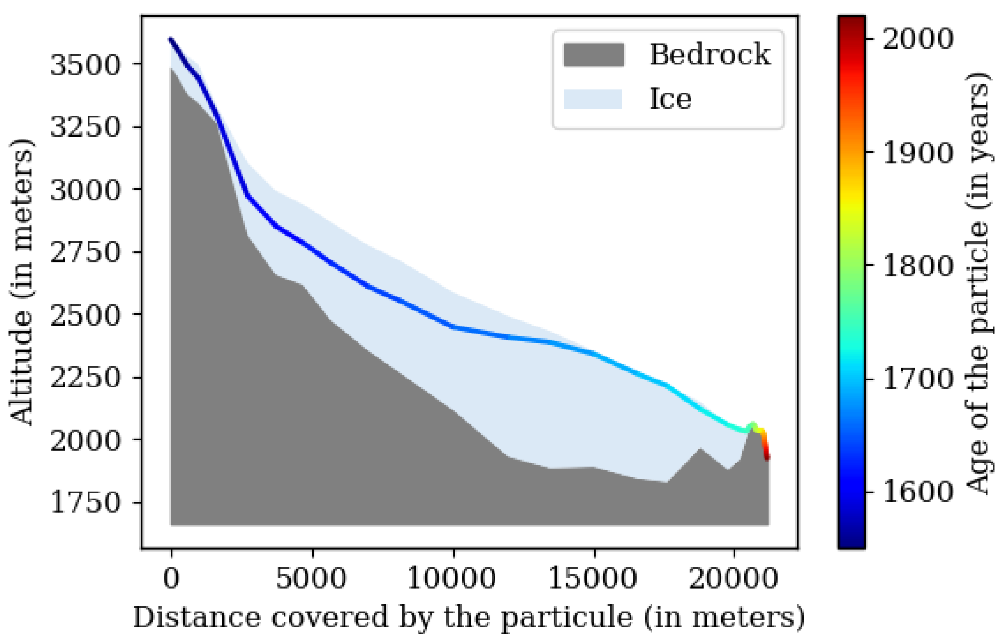

Figure 21: Trajectory of a particle in Aletsch glacier with incompressibility method